

## Electron density of states of CdTe

A. Wall,\* Y. Gao,<sup>†</sup> A. Raisanen, A. Franciosi, and James R. Chelikowsky

*Department of Chemical Engineering and Materials Science, University of Minnesota, Minneapolis, Minnesota 55455*

(Received 11 May 1990; revised manuscript received 1 October 1990)

We present bremsstrahlung-isochromat-spectroscopy and synchrotron-radiation photoemission-spectroscopy studies of CdTe single crystals cleaved *in situ*. The photoemission data, and empirical-pseudopotential calculations of the band structure, were used to reevaluate the position of valence and core spectral features. The bremsstrahlung-isochromat-spectroscopy results emphasize structure in the conduction-band density of states at 4.1, 6.7, 9.6, 11.3, 12.5, and 15 eV above the valence-band maximum. The calculations are found to reproduce the conduction-band structure throughout a range of 18 eV above the valence-band maximum.

### I. INTRODUCTION

The prototypical II-VI semiconductor CdTe has been the focus of a number of pioneering photoemission-spectroscopy investigations.<sup>1-3</sup> More recently a number of proposed optoelectronic device applications have stimulated strong interest in the properties of metal-CdTe contacts,<sup>4-7</sup> and CdTe-based II-VI heterojunction systems.<sup>8-13</sup> Most photoemission interface studies of this type rely on the behavior of well-recognizable density-of-states (DOS) features to extract information on CdTe chemistry or electrostatics. However, no recent comprehensive study of CdTe valence- and conduction-band DOS features, *vis-à-vis* state-of-the-art calculations, is available, to our knowledge. We study here the electronic structure of CdTe with special emphasis on the position of the major DOS features as determined both experimentally and theoretically. We employed a combination of synchrotron-radiation photoemission spectroscopy and inverse-photoemission spectroscopy<sup>14,15</sup> in the bremsstrahlung-isochromat-spectroscopy (BIS) mode on CdTe(110) samples cleaved *in situ*, together with empirical-pseudopotential calculations of the bulk band structure.

Our photoemission data, including a deconvolution of the shallow surface and bulk-related Cd *4d* core levels as a function of photon energy, indispensable to extract reliably the Te *5s* contribution, were compared with existing semiempirical DOS calculations.<sup>16</sup> Remarkably good agreement was found between theoretical and experimental features, including the cation- and anion-derived *s* features which had received comparatively little attention in the past.

We employed BIS at 1486.6 eV to examine the total density of states in the conduction bands within 18 eV of the valence-band maximum  $E_v$ . Comparison with the results of our semiempirical-pseudopotential calculations of the conduction bands, obtained following the methodology and extending the results of Chelikowsky and Cohen,<sup>16</sup> showed remarkable quantitative agreement. The agreement is especially comforting in view of the limited amount of experimental information about the

optical gaps used for the empirical corrections to the pseudopotential, and considering the predicted limitations of the local-density approximation for describing conduction-band states.

### II. EXPERIMENTAL DETAILS

Bulk single-crystal samples of CdTe were placed in an analysis chamber at operating pressures in the  $10^{-11}$ -Torr range. Atomically clean surfaces were obtained by cleaving the samples *in situ*. The cleaved surfaces ranged from stepped surface to flat mirrorlike (110) cleavage surfaces, but the results discussed here are all independent of cleave quality and reflect bulklike electronic properties.<sup>17</sup>

The photoemission measurements were performed by positioning the cleaved surface at the common focus of a monochromatic synchrotron-radiation beam and a commercial hemispherical electron-energy analyzer. Synchrotron radiation from the 800-MeV electron-storage ring Aladdin at the Synchrotron Radiation Center of the University of Wisconsin-Madison was dispersed with a 3-m toroidal grating monochromator. Energy-distribution curves (EDC's) were collected in the  $15 \text{ eV} \leq h\nu \leq 120 \text{ eV}$  photon-energy range. The overall energy resolution (electron plus photon) was 0.15 eV for the lowest photon energies, and 0.45 eV for the largest values of  $h\nu$ , as measured from the width  $dE_F$  of the Fermi level  $E_F$  of a thick metallic film (Mn or Pd) deposited *in situ* onto the sample.<sup>18</sup>

BIS studies of the unoccupied DOS were also performed on surfaces cleaved *in situ*. A Pierce-type electron gun was used to form and focus onto the surface a monochromatic electron beam with kinetic energies of 1480–1510 eV. As the electron kinetic energy was varied, x-ray photons emitted with  $h\nu = 1486.6 \text{ eV}$  were selected by means of a 0.5-m Rowland circle quartz grating monochromator and detected with a microchannel plate. The resulting isochromat spectra were then averaged for 18–20 different cleaves. Details of the experimental system can be found in Ref. 19. The overall energy resolution of the BIS measurements was determined as 0.7 eV from the Fermi-level-energy width  $dE_F$  (Ref. 18)

in the isochromat spectra from thick Pd films deposited *in situ* onto the samples.

### III. RESULTS AND DISCUSSION

#### A. Valence-band density of states

High-resolution EDC's for the valence-band emission from CdTe are shown in Fig. 1. In Fig. 1(a) we show an EDC at  $h\nu=60$  eV (solid line) together with earlier x-ray photoemission (XPS) results<sup>8</sup> for CdTe(111) (dashed line). The binding energies are referred to the valence-band maximum  $E_v$ . We elected to compare our results with those of Ref. 8 because of the highly accurate method used to determine the position of the valence-band maximum  $E_v$ . Structure in the 8–12-eV range reflects mostly the Cd 4*d* core emission. In Fig. 1(b) (dash-dotted line) is the calculated DOS from Ref. 16, and the same DOS convoluted with a Gaussian function [full width at half maximum (FWHM) = 0.4 eV, solid line]. There is general agreement between the two experimental spectra, although our higher-resolution results seem to put the valence-band maximum some 0.25 eV closer to valence and core emission features, and show a well-defined shoulder on the low-binding-energy side of the 4*d* cores in the 8–12-eV range. These differences are the result of the improved energy resolution and higher surface sensitivity of our data. We will show that the apparent shift of the Cd 4*d* core levels, for example, is due to the greater surface-related Cd 4*d* contribution in our results, and that the low-binding-energy shoulder corresponds to a Te 5*s* DOS feature which is visible in our higher-resolution results.

Except for the different experimental resolution and photon energy employed, the position of  $E_v$  was determined with a similar procedure here and in Ref. 8. The procedure involves a least-squares fit of the experimental data to a suitable broadened theoretical density of states in the region of the leading valence-band edge.<sup>13</sup> The position of the theoretical DOS versus the experimental spectrum and the location of  $E_v$  was determined by fitting within an energy window that includes the valence-band edge.<sup>20</sup>

For fitting windows extending more than about 1.0 eV below the valence-band maximum, the position of  $E_v$  is independent of the Gaussian width within experimental uncertainty ( $\pm 0.05$  eV). Thus as the fitting window includes more of the data, the choice of Gaussian FWHM becomes less important. The average position of  $E_v$  that would be obtained from a linear extrapolation of the leading edge, a method often used during heterojunction band-offset measurements, would be, instead, dependent on the size of the fitting window and, in especially unfortunate cases, could place the edge as much as 0.3 eV too deep in the valence band. This could affect the calculated value of a heterojunction valence-band offsets in those cases in which the linear extrapolation method is employed, and the other semiconductor involved has a qualitatively different leading valence-band edge. A heterojunction such as HgTe-CdTe (Ref. 21), for example, would be less likely to be affected than Si-CdTe,<sup>22</sup> because the DOS near  $E_v$  is mostly Te *p* derived for both HgTe

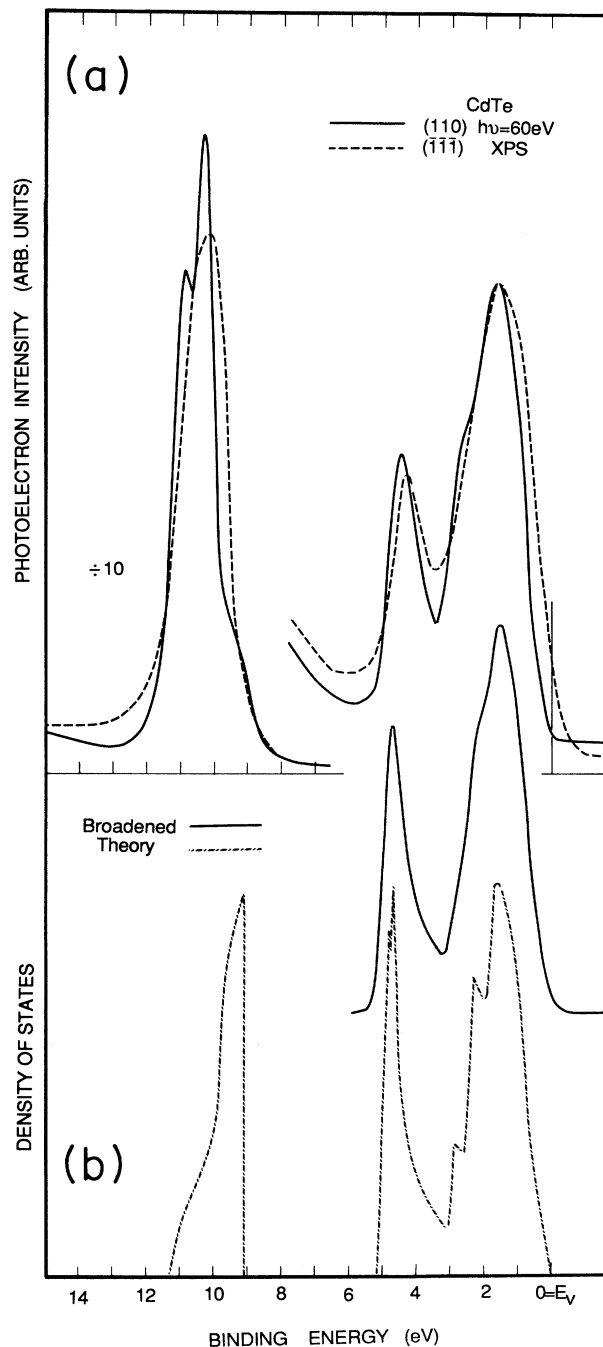


FIG. 1. (a) Photoelectron energy distribution curve (EDC) for the valence band and shallow core emission from CdTe(110) at  $h\nu=60$  eV (solid line). The Cd 4*d* core levels (9–12 eV) are shown in a reduced scale. The binding energy is referred to the valence-band maximum  $E_v$ . Superimposed on this spectrum is an EDC for the valence-band emission obtained in Ref. 8 through x-ray photoemission (XPS) studies of molecular beam epitaxy grown CdTe(111) (dashed line). (b) Theoretical electron density of states (DOS) for CdTe from the nonlocal pseudopotential calculations of Ref. 16 (dash-dotted line). To facilitate comparison with the experimental EDC, we also show the theoretical DOS convoluted (solid line) with a Gaussian function with full width at half maximum (FWHM) = 0.4 eV.

and CdTe. Schottky barrier measurements should not be affected in those cases in which semiconductor core-level shifts are used to monitor band bending and barrier formation and the semiconductor is in flat-band conditions prior to metal deposition.<sup>4</sup> A detailed exam of these interface issues, however, is beyond the scope of this work, which focuses on the comparison of experiment and theory for the DOS of CdTe.<sup>23</sup>

Relative to the position of  $E_v$ , major features in the valence-band DOS include Te 5*p*-derived structure with a maximum at  $1.65 \pm 0.05$  eV and extending 3.4 eV below  $E_v$ , structure at  $0.90 \pm 0.05$  eV corresponding to the spin-orbit-split valence band at  $\Gamma$ , and a shoulder at 2.7 eV due to emission from states between *K* and  $\Gamma$  in the Brillouin zone, all in good agreement with the calculations. The second experimental DOS feature at  $4.50 \pm 0.05$  eV corresponds to emission from Cd *s*-Te *p* hybrid levels with  $L_6$  symmetry that the theory places at  $4.7 \pm 0.1$  eV. Previous XPS results in Fig. 1 (dashed line) yielded a value of  $4.3 \pm 0.1$  eV for this feature, possibly due to the poorer experimental resolution, which tends to broaden preferentially the spectral feature on the low-binding-energy side because of the additional Te *p* contribution.

The determination of the Te 5*s* contribution to the bulk CdTe DOS is somewhat complicated by the partial superposition with the Cd 4*d* core levels. An examination of the most recent literature on the subject reveals contrasting results. In a study of sputter-cleaned CdTe(100) John *et al.* reported<sup>7</sup> the existence of two surface-related Cd 4*d* doublets, one on either side of the bulk-related Cd 4*d* doublet. The Te 5*s* contribution is notably absent. Conversely, Prince *et al.*,<sup>24</sup> in a study of CdTe(110) cleaved *in situ*, published two spectra (for the same photon energy of 50 eV and two different photoelectron emission angles) in which the photoemission features in the 8–12-eV range were decomposed in terms of a bulk-related Cd 4*d* doublet, a surface-related 4*d* doublet, and a Te 5*s* contribution.

In order to determine unambiguously the Te 5*s* contribution to the DOS we performed systematic deconvolutions of the spectral features of interest throughout the 40–95-eV photon energy range, examining the possible existence of up to three Cd 4*d* doublets and a Te 5*s* contribution. The best fits consistently showed the presence of only two Cd 4*d* doublets. A representative deconvolution of the Cd 4*d* and Te 5*s* DOS features is shown in Fig. 2 for a photon energy of 50 eV. The data (solid circles) are shown together with the results of a best fit of the spectrum (solid line) in terms of three different contributions (also shown, dashed line). The component at the center of Fig. 2 derives from bulk Cd 4*d* core emission, with  $j = \frac{5}{2}$  and  $j = \frac{3}{2}$  spin-orbit-split subcomponents. To the left of the bulk Cd 4*d* doublet is a surface-related 4*d* doublet, and to the right a Te 5*s* DOS feature. The secondary-electron background is also shown as a smooth dashed line at the bottom. The deconvolution in Fig. 2 was obtained using Lorentzian line shapes convoluted with a Gaussian function for each Cd 4*d* subcomponent and the Te 5*s* feature (i.e., a total of five spectral features). A least-squares fitting procedure was used to determine

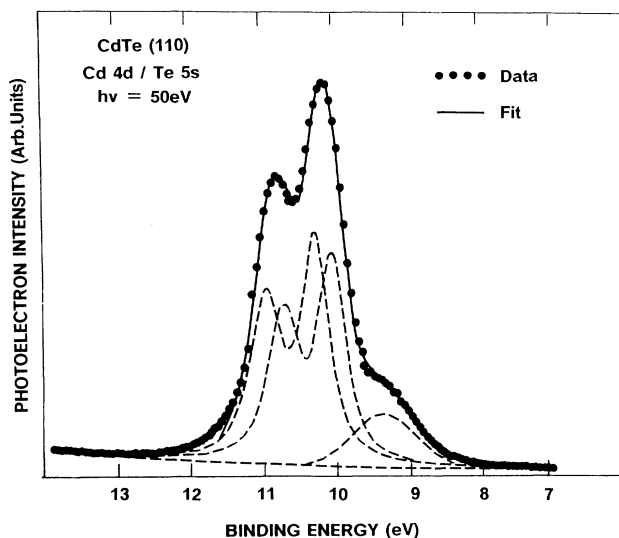


FIG. 2. EDC for CdTe(110) in the 8–13-eV binding energy range below the valence-band maximum  $E_v$ , at a photon energy of 50 eV (solid circles). A best fit of the overall line shape (solid line) was obtained through a least-squares procedure described in the text. Three different components (dashed lines) correspond to the dominant Cd 4*d* bulk core doublet, a surface-related Cd 4*d* doublet shifted to higher binding energy by 0.22 eV, and a Te 5*s*-derived valence-band feature at 9.22 eV below the valence-band maximum  $E_v$ .

position, intensity, and Gaussian and Lorentzian width of the different subcomponents. Typical values of the fitting parameters at  $h\nu = 50$  eV are in good quantitative agreement with those obtained by Prince *et al.*<sup>24</sup> at the same photon energy (Ref. 25). Representative values of the fitting parameters throughout the  $40 \leq h\nu \leq 95$  eV range are listed in Ref. 26.

Our photon-energy-dependent results indicate that a single surface-related Cd 4*d* doublet shifted by  $0.22 \pm 0.03$  eV to a higher binding energy relative to the bulk-related doublet (bulk  $4d_{5/2}$  component at  $10.10 \pm 0.05$  eV) is observed at all photon energies explored. The photon energy dependence of the photoemission cross section fully supports the surface-related origin of this feature, and from the relative intensity of the two doublets we can also directly estimate the photoelectron escape depth in CdTe as a function of photon energy (see Ref. 27). We note that the bulk Cd  $4d_{5/2}$  position at  $10.10 \pm 0.05$  eV is consistent with the position of the main 4*d* feature observed in the XPS results of Ref. 8 (Fig. 1, dashed line) as expected because of the lower surface sensitivity of the XPS data.

As a result of our deconvolution we consistently obtain the Te 5*s* contribution as a Voigt-like line shape centered at  $9.22 \pm 0.10$  eV with a FWHM of about 1 eV and exhibiting relatively little dispersion with photon energy. This is in remarkable quantitative agreement with the results of the semiempirical calculations by Chelikowsky and Cohen,<sup>16</sup> which show a 5*s*-derived feature at 9.2 eV, with a FWHM of 1.0 eV. Fairly good agreement is found with

earlier Korringa-Kohn-Rostocker muffin-tin potential calculations by Eckelt.<sup>28</sup>

### B. Conduction-band density of states

Many first-principles calculation techniques encounter difficulty when considering the unoccupied density of states above the Fermi level in semiconductors. For instance, attempts to treat exchange and correlation effects in the local-density approximation typically result in semiconductor band gaps that are 40–60% too small.<sup>29</sup> In the semiempirical nonlocal pseudopotential method these effects are corrected through comparison with experimental optical absorption data at critical points. We have extended the calculations of Ref. 16 to a range of 18 eV above the valence-band maximum, in order to facilitate interpretation of our BIS measurements. The resulting band structure along the  $\Lambda$  and  $\Delta$  directions in the Brillouin zone is shown in Fig. 3(a). The corresponding

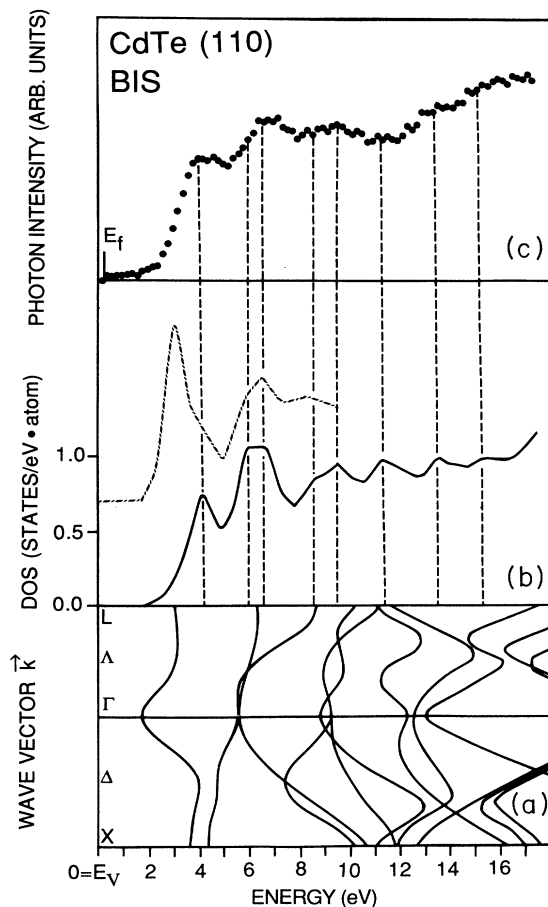


FIG. 3. (a) Conduction bands for CdTe in the  $\Lambda$  and  $\Delta$  directions of the Brillouin zone as calculated through the nonlocal semiempirical pseudopotential method of Ref. 16. (b) The total DOS for the conduction bands of CdTe as calculated from the bands shown in (a) (solid line) is compared with earlier inverse photoemission results for CdTe(110) (dash-dotted line, from Ref. 30 at an incident electron energy of 16.25 eV). (c) Bremsstrahlung-isochromat-spectroscopy (BIS) results for CdTe, from this work. The dashed lines mark the position of the major features in the theoretical DOS of (a).

density of states is shown in Fig. 3(b) with zero of the binding energy scale referred to the valence-band maximum  $E_v$ .

Representative BIS data for cleaved CdTe are shown in Fig. 3(c). DOS features give rise to structure in the spectrum superimposed on a smoothly increasing secondary photon background resulting from the decay of inelastically scattered electrons. The spectrum in Fig. 3(c) was obtained as the sum of several quantitatively consistent spectra from different cleaves, and corresponds to a total of some 150 h of data integration with a primary electron beam current of approximately 200  $\mu$ A. We observed no electrostatic sample charging at such current levels. A new cleave was prepared every six to eight hours to prevent electron-beam-induced contamination. The major experimental features in Fig. 3(c) have been aligned with structure in the calculated DOS [Fig. 3(b)]. The resulting rigid shift was  $<0.2$  eV, so that the position of  $E_v$  in Fig. 3(c) is within 0.2 eV of the  $E_v$  location obtained by equating the Fermi-level position  $E_F$  in the BIS and photoemission data ( $E_F - E_v = 0.47$  eV in Fig. 1). The small correction necessary for the alignment could in principle be related to differences between the photoemission final state and the optical absorption final state which intervenes in the determination of the semiempirical pseudopotential. However, a more likely explanation derives from the experimental uncertainty in the relative position of photoemission and BIS spectra. The combined uncertainty is determined by the uncertainty in the position of the photoemission- ( $dE_F = 0.3$  eV) and BIS-determined ( $dE_F = 0.7$  eV) Fermi levels, and therefore exceeds the rigid shift employed in Fig. 3 ( $<0.2$  eV).

Both the BIS spectrum and the calculated DOS in Fig. 3 indicate that the conduction-band minimum appears as the end point of a “tailing” of states extending to about 1.5 eV (band gap  $E_g = 1.56$  eV). The first peak in the BIS data of CdTe appears at approximately 4.1 eV above  $E_v$ , and corresponds to the position of the first DOS feature in our calculations. This feature originates from states in the first two conduction bands along  $\Delta$  and near  $X$  in the Brillouin zone [Fig. 3(a)]. The second peak in the data [Fig. 3(c)] appears centered at  $6.7 \pm 0.3$  eV above  $E_v$ , and the theoretical density of states exhibits a major DOS feature at 6.5 eV. The calculation indicates that a major contribution to this DOS feature derives from states in low symmetry directions of the Brillouin zone. A double emission feature in the BIS spectrum extends from approximately 8 to 10 eV with a maximum at 9.6 eV. The calculated density of states exhibits a double structure in this energy range (with a maximum at 9.5 eV), originating from states in the third conduction band at  $L$  (approximately 8.7 eV) and from a combination of states from higher bands in the  $\Lambda$  direction (contributing to the 9.5-eV maximum). The BIS spectrum displays small features on the smooth backgrounds at approximately 11.3 and 12.5 eV which also correspond to structure in the theoretical DOS electron bands throughout  $k$  space contribute to these high-energy features as the bands become increasingly free-electron-like. A density-of-states feature appearing in the calculation at approximately 15 eV corresponds to weak structure in the BIS spectrum,

but the low intensity of this feature relative to the background prevents an unambiguous identification.

The only major theoretical DOS feature not clearly observed in the BIS spectrum is at approximately 6 eV above the valence band maximum [Fig. 3(b)] and was instead observed in inverse photoemission studies of CdTe(110) at ultraviolet photon energies.<sup>30</sup> A spectrum from that work at a primary-electron energy of 16.25 eV is shown for comparison in Fig. 3(b) (dash-dotted line). The ultraviolet spectrum also exhibits a dominant feature at about 3 eV, ascribed<sup>30</sup> to an unoccupied surface resonance. Both the 3- and the 6-eV features decrease in intensity with increasing electron energy and are absent in our x-ray results. BIS matrix elements will have to be calculated explicitly to explain this energy dependence.

The good agreement between the BIS data and the calculations was expected for the lowest DOS features, since the semiempirical pseudopotential method uses reflectivity data to fix the lowest band energies at critical points. However, the theory appears to go well beyond such expectations and successfully reproduce all of the observed inverse-photoemission features.

#### IV. CONCLUSIONS

We have reexamined the electronic density of states of CdTe with a combination of high-resolution synchrotron-radiation photoemission spectroscopy and bremsstrahlung-isochromat spectroscopy. The position of the valence-band maximum  $E_v$  was determined through a least-squares fit to a theoretical density of

states. We found a bulk Cd  $4d_{5/2}$  binding energy of  $10.10 \pm 0.05$  eV (spin-orbit splitting  $0.68 \pm 0.05$  eV), and a single Cd  $4d$  surface doublet shifted  $0.22 \pm 0.04$  eV to higher binding energy relative to the bulk Cd  $4d$  core emission. A deconvolution of the Cd  $4d$  line shape yields a valence-band density of states feature with Te  $5s$  character  $9.22 \pm 0.10$  eV below  $E_v$ . Agreement between experiment and the results of semiempirical-nonlocal-pseudopotential calculations is remarkably good, for both the valence states and the conduction bands. In particular, BIS measurements are in good quantitative agreement with theory throughout the 18-eV energy range explored, notwithstanding the relatively small amount of experimental reflectivity information that was used in the determination of the empirical pseudopotential.

#### ACKNOWLEDGMENTS

This work was supported in part by the Office of Naval Research under Grant No. N00014-89-J-1407 and by the Center for Interfacial Engineering at the University of Minnesota. One of us (J.R.C.) would like to thank the Minnesota Supercomputer Institute for computational support. We thank J. H. Weaver for the use of the BIS spectrometer and J. K. Furdyna for providing us with the crystals used in this study. The crystal growth was performed at Purdue University and supported by the National Science Foundation (NSF). Finally, we wish to thank the staff of the University of Wisconsin Synchrotron Radiation Center, supported by the NSF, for their expert and cheerful support.

\*Present address: IBM Corporation, Rochester, MN 55901.

†Present address: Department of Physics and Astronomy, University of Rochester, Rochester, NY 14627.

<sup>1</sup>N. J. Shevchik, J. Tejada, M. Cardona, and D. W. Langer, *Phys. Status Solidi B* **59**, 87 (1973).

<sup>2</sup>D. E. Eastman, W. D. Grobman, J. L. Freeouf, and M. Erbudak, *Phys. Rev. B* **9**, 3473 (1974).

<sup>3</sup>L. Ley, R. A. Pollak, F. R. McFeely, S. P. Kowalczyk, and D. A. Shirley, *Phys. Rev. B* **9**, 600 (1974).

<sup>4</sup>L. J. Brillson, *Surf. Sci. Rep.* **2**, 123 (1982), and references cited therein.

<sup>5</sup>M. H. Patterson and R. H. Williams, *J. Cryst. Growth* **59**, 281 (1982).

<sup>6</sup>D. J. Friedman, I. Lindau, and W. E. Spicer, *Phys. Rev. B* **34**, 5329 (1986); **37**, 731 (1988).

<sup>7</sup>P. John, T. Miller, T. C. Hsieh, A. P. Shapiro, A. L. Wachs, and T. C. Chiang, *Phys. Rev. B* **34**, 6704 (1986).

<sup>8</sup>S. P. Kowalczyk, J. T. Cheung, E. A. Kraut, and R. W. Grant, *Phys. Rev. Lett.* **56**, 1605 (1986).

<sup>9</sup>G. Margaritondo and A. Franciosi, *Annu. Rev. Mater. Sci.* **14**, 67 (1984); F. Capasso and G. Margaritondo, *Heterojunction Band Discontinuities, Physics and Device Applications* (North-Holland, Amsterdam, 1987).

<sup>10</sup>P. Perfetti, F. Patella, F. Sette, C. Quaresima, C. Capasso, A. Savoia, and G. Margaritondo, *Phys. Rev. B* **29**, 5941 (1984).

<sup>11</sup>J.-P. Faurie, C. Hsu, and T. M. Duc, *J. Vac. Sci. Technol. A* **5**, 3074 (1987).

<sup>12</sup>X. Yu, A. Wall, A. Raisanen, G. Haugstad, G. Ceccone, N.

Troullier, and A. Franciosi, *Phys. Rev. B* **42**, 1872 (1990).

<sup>13</sup>E. A. Kraut, R. W. Grant, J. R. Waldrop, and S. P. Kowalczyk, *Phys. Rev. Lett.* **44**, 1620 (1980); *Phys. Rev. B* **28**, 1965 (1983).

<sup>14</sup>F. J. Himpsel and Th. Fauster, *J. Vac. Sci. Technol. A* **2**, 815 (1984); P. D. Johnson and N. V. Smith, *Phys. Rev. B* **27**, 2527 (1983); N. V. Smith, *Rep. Prog. Phys.* **51**, 1227 (1988).

<sup>15</sup>J. R. Chelikowsky, T. J. Wagener, J. H. Weaver, and A. Jin, *Phys. Rev. B* **40**, 9644 (1989).

<sup>16</sup>J. R. Chelikowsky and M. L. Cohen, *Phys. Rev. B* **14**, 556 (1976); M. L. Cohen and J. R. Chelikowsky, *Electronic Structure and Optical Properties of Semiconductors* (Springer-Verlag, Heidelberg, 1988).

<sup>17</sup>With the obvious exception of the surface-related Cd  $4d$  doublet, to be discussed in what follows.

<sup>18</sup> $dE_F$  was obtained as the energy separation between the intercepts of a linearly interpolated Fermi cutoff with linear extrapolations of the secondary background on the low-binding-energy side, and of the valence band DOS on the high-binding-energy side. This corresponded (within experimental uncertainty) to the energy separation of the two points at which the emission intensity achieved 10% and 90%, respectively, of the maximum emission intensity near  $E_F$ . A similar method was used to define  $dE_F$  in the BIS measurements.

<sup>19</sup>Y. Gao, M. Grioni, B. Smandek, J. H. Weaver, and T. Tyrie, *J. Phys. E* **21**, 489 (1988).

<sup>20</sup>Crucial parameters are the choice of the FWHM of the broadening function and the size of the fitting window. We

- used a direct measurement of the Fermi-level width  $dE_F$  (Ref. 18) to determine the FWHM and monitored the quality of the fit from the total square deviation per point (TSQ) and from the position of  $E_v$  (corresponding to the minimum TSQ) as a function of how far the fitting window extended into the valence band. Physically meaningful results always corresponded to a wide range of window sizes where the TSQ and the position of  $E_v$  were constant.
- <sup>21</sup>S. P. Kowalczyk, J. T. Cheung, E. A. Kraut, and R. W. Grant, *Phys. Rev. Lett.* **56**, 1605 (1986); T.-M. Duc, C. Tsu, and J. P. Faurie, *ibid.* **58**, 1127 (1987).
- <sup>22</sup>G. Margaritondo, in *Heterojunction Band Discontinuities, Physics and Device Applications*, edited by F. Capasso and G. Margaritondo (North-Holland, Amsterdam, 1987).
- <sup>23</sup>A discussion of selected CdTe interface issues will be presented elsewhere: L. Vanzetti, A. Wall, X. Yu, G. Ceccone, G. Bratina, and A. Franciosi (unpublished).
- <sup>24</sup>K. C. Prince, G. Paolucci, V. Chab, M. Surman, and A. M. Bradshaw, *Surf. Sci.* **206**, L871 (1988).
- <sup>25</sup>Line-shape parameters obtained from our fitting procedure (Fig. 2) can be directly compared with those obtained by Prince *et al.* at the same photon energy (50 eV) in Ref. 24 (given in parentheses): Cd 4*d* bulk doublet: spin-orbit splitting = 0.68 eV (0.68 eV), branching ratio = 0.64, Gaussian FWHM = 0.41 eV (0.37 eV), Lorentzian FWHM = 0.22 eV (0.25 eV). Cd 4*d* surface doublet: spin-orbit splitting = 0.68 eV (0.68 eV), branching ratio = 0.66, Gaussian FWHM = 0.41 eV (0.37 eV), Lorentzian width = 0.22 eV (0.25 eV), surface shift = -0.22 eV (-0.24 eV). Te 5*s* DOS feature: Gaussian FWHM = 0.62 eV (0.5 eV), Lorentzian FWHM = 0.42 eV (0.75 eV), shift relative to the bulk 4*d*<sub>5/2</sub> level = 0.77 eV.
- <sup>26</sup>Spin-orbit splitting and branching ratios of the two Cd 4*d* doublets were consistent with those at  $h\nu=50$  eV throughout the whole photon energy range explored. The Cd 4*d* surface to bulk intensity ratio  $S_b$  and the Te 5*s* to bulk Cd 4*d* intensity ratio  $T_b$  at representative photon energies were  $h\nu=40$  eV,  $S_b=0.78\pm0.08$ ,  $T_b=0.06\pm0.03$ ;  $h\nu=45$  eV,  $S_b=1.11\pm0.10$ ,  $T_b=0.15\pm0.07$ ;  $h\nu=50$  eV,  $S_b=1.09\pm0.10$ ,  $T_b=0.25\pm0.07$ ;  $h\nu=60$  eV,  $S_b=0.67\pm0.07$ ,  $T_b=0.15\pm0.04$ ;  $h\nu=95$  eV,  $S_b=0.35\pm0.07$ ,  $T_b=0.02\pm0.04$ .
- <sup>27</sup>From the Cd 4*d* surface to bulk intensity ratio  $S_b$ , the photoelectron escape depth  $\lambda$  can be estimated using the method by J. F. van der Veen, F. J. Himpsel, and D. E. Eastman, *Phys. Rev. Lett.* **44**, 189 (1980). In our experimental geometry photoelectrons were collected at an average takeoff angle of 45°, so that the experimental value of the  $S_b$  reflects an effective escape depth  $L=\lambda\cos\theta$ . In what follows we give values of  $\lambda$  at different photon energies  $h\nu$  for Cd 4*d* photoelectrons:  $h\nu=40$  eV,  $\lambda=5.6\pm0.6$  Å;  $h\nu=45$  eV,  $\lambda=4.3\pm0.4$  Å;  $h\nu=50$  eV,  $\lambda=4.4\pm0.4$  Å;  $h\nu=60$  eV,  $\lambda=6.4\pm0.6$  Å;  $h\nu=95$  eV,  $\lambda=10.8\pm1.1$  Å. We note that our result for  $\lambda$  at  $h\nu=50$  eV is consistent with that of  $5\pm2$  Å reported by Prince *et al.* in Ref. 24.
- <sup>28</sup>P. Eckelt, *Phys. Status Solidi* **23**, 307 (1967).
- <sup>29</sup>B. E. Larson, K. C. Hass, H. Ehrenreich, and A. E. Carlsson (unpublished); M. S. Hybertsen and S. G. Louie, *Phys. Rev. B* **35**, 5602 (1987).
- <sup>30</sup>K. O. Magnusson, U. O. Karlsson, D. Straub, S. A. Flodstrom, and F. J. Himpsel, *Phys. Rev. B* **36**, 6566 (1987).